SUPPLEMENTAL MATERIAL

1. SUPPLEMENTAL METHODS

1A. Myocardial apoptosis detection- immunofluorescence microscopy. Using a rat heart slicer matrix, 1-mm axial sections were cut, fixed in 1% formalin, paraffin embedded, and cut into 12-μm sections.

Terminal deoxynucleotidyl transferase dUTP nick end labeling (TUNEL) assay was used to detect apoptosis in LV myocardial tissue, according to the manufacturer's instructions (Roche Diagnostics, Indianapoils, IN). In brief, after deparaffinization, sections were pretreated with 0.1 M citrate buffer (pH 6) in a 350-watt microwave oven for 5 minutes. Sections were then incubated with a fluorescein-TUNEL reaction mixture for 1 hour at 37°C in order to label apoptotic cells. After rinsing with PBS, the slides were mounted with DAPI (Santa Cruz). The apoptotic cells appeared green under a fluorescence microscope (Leica DM IRB, Germany) using a 20X/1.5 Plain objective. A negative control was incubated with label solution (without terminal transferase) instead of the TUNEL reaction mixture. The total numbers of both TUNEL-positive and DAPI-positive cells were recorded in 5 representative areas of the myocardium, and expressed as %TUNEL positive nuclei.

Confocal microcopy: to determine the abundance of apoptotic cardiomyocytes, double immunofluorescence staining for active caspase-3 and troponin I was performed in FFPE heart sections. After deparaffinization, the sections were treated with 10 mM citrate buffer (pH 6.0) for permeabilization. After blocking with 10% goat serum for 60 minutes at room temperature, sections were incubated with rabbit anti-cleaved caspase-3 antibody (1:200, Cell Signaling) and mouse anti-troponin I (C-4, 1:500, Santa Cruz,) at 4°C overnight. Sections were then incubated separately with Alexa Fluor 550-conjugated goat anti-mouse IgG (Invitrogen; 1:500) and Alexa Fluor 488-conjugated goat anti-rabbit IgG (Invitrogen; 1:500) for 60 minutes at room temperature. Images were captured on a Leica SP5 confocal microscope (Leica Microsystems) using a 40X/1.25-0.75 Plain APO oil objective.

1.B. Sample preparation and protein isolation for mass spectrometry. Snap frozen LV myocardium samples from AGS and rats were processed at the Duke Proteomics Shared Resource. Each piece of tissue was weighed and subjected to a Trizol based solubilization protocol written by Thompson and Foster (available at *http://www.genome.duke.edu/cores/proteomics/samplepreparation/documents/TRIzolTissueHomogenizationandProteinExtraction.pdf*). Following resuspension in 200 uL 50mM ammonium bicarbonate/ 0.25% ALS-1 (standard MS-compatible surfactant), all samples were subjected to a micro Bradford assay (Pierce) to measure total protein concentration. 50 ug from each sample was then removed and normalized to 0.55 ug/ul in uL 50 mM ammonium bicarbonate, pH 8 with 0.25% ALS-1 (standard MS-compatible surfactant). Samples were reduced (10 mM DTT), cysteine alkylated (20 mM iodoacetamide), and trypsin digested according to the DPCF standard protocol (available at *http://www.genome.duke.edu/cores/proteomics/sample-preparation/documents/InsolutionDigestionProtocol_012309.doc*). After digestion, all samples were spiked with ADH1_YEAST digest (Massprep standard, Waters Corporation) as a surrogate standard (20 fmol ADH per ug soluble myocardium protein), were taken to dryness and resuspended in 200 mM ammonium formate (pH 10.0) at a concentration of 1 ug/ul prior to 5-fraction LC-LC-MS analysis. In addition to the 38 individual samples, a QC pool was created from equal portions of all 38 samples. This QC pool was run approximately once a day to assess technical variability in measured protein quantity across the total acquisition window (~12 days).

1.C. Quantitative proteomic analysis of AGS and rat myocardium. Quantitative two-dimensional liquid chromatography – tandem mass spectrometry (LC/LC-MS/MS) was performed on 3 μg of protein digest per sample in singlicate. The method uses 2D liquid chromatography in a high-low pH reversed phase/reversed phase configuration on a nanoAcquity UPLC system (Waters Corp.) coupled to a Synapt G2 HDMS high resolution accurate mass tandem mass spectrometer (Waters Corp.) with nanoelectrospray ionization in a manner similar to previously described.[1-3] Peptides were first trapped at 2 μl/min at 97/3 v/v water/MeCN in 20 mM ammonium formate (pH 10) on a 5 μm XBridge BEH130 C18 300 um Å~ 50 mm column (Waters). A series of step-elutions of MeCN at 2 μl/min was used to elute peptides from the 1st dimension column. Ten steps of 7.4%, 10.8%, 12.6%, 14.0%, 15.3%, 16.7%, 18.3%, 20.4%, 23.5%, and 50.0% MeCN were utilized for

the unbiased analyses; these percentages were optimized for delivery of an approximately equal load to the 2nd dimension column for each fraction. For 2nd dimension separation, the eluent from the 1st dimension was first diluted 10-fold online with 99.8/0.1/0.1 v/v/v water/MeCN/formic acid and trapped on a 5µm Symmetry C18 180 µm Å~ 20 mm trapping column (Waters). The 2nd dimension separations were performed on a 1.7 µm Acquity BEH130 C18 75 µm Å~ 150 mm column (Waters) using a linear gradient of 7 to 35% MeCN with 0.1% formic acid over 37 min, at a flow rate of 0.5 µl/min and column temperature of 35 °C. Data collection on the Synapt G2 mass spectrometer was performed in ion-mobility assisted data-independent acquisition (HDMSE) mode, using 0.6 second alternating cycle time between low (6V) and high (27-50V) collision energy (CE). Scans performed at low CE measure peptide accurate mass and intensity (abundance), while scans at elevated CE allow for qualitative identification of the resulting peptide fragments via database searching. The total analysis cycle time for each sample injection was approximately 6 hours.

Samples were run in a randomized order, with the exception of the QC Pools, which were run once every 7th injection. Following the 46 analyses, data was imported into Rosetta Elucidator v3.3 (Rosetta Biosoftware, Inc) and three different experimental definitions were created; one with all the QC pool samples, one with all the rat samples and one with all the AGS samples. Within each experimental definition, LC/LC-MS runs were aligned based on the accurate mass and retention time of detected ions ("features") using PeakTeller algorithm (Elucidator). The relative peptide abundance was calculated based on area-under-the-curve (AUC) of aligned features across all runs. The QC pool, rat, and AGS datasets had 561504, 627409, and 767434 quantified features, respectively, and high collision energy (peptide fragment) data were collected in 278771, 952316, and 1621914 spectra, respectively, for sequencing by database searching.

This MS/MS data for rat samples were searched against an NCBI RefSeq_Rattus database created on 11/30/2012 (25,485 forward entries). The MS/MS data for AGS samples was searched against a curated AGS database representing refined thirteen-lined ground squirrel (*Ictidomys tridecemlineatus*) and human protein sequences from Ensembl release 69, as described in detail below.

1.C.1. Refinement of protein sequences for Arctic Ground Squirrel

Protein sequences of thirteen-lined ground squirrel (*Ictidomys tridecemlineatus*, TGS) were translated from Ensembl known or novel gene predictions of genome assembly Spetri2 (Nov 2011, Ensembl release 69). In total, 20,000 protein sequences with a length of 513 (SD ±483) were downloaded. 101,075 sequences of human protein with length 383 (SD ±504) were downloaded from genome assembly GRCh37 (Ensembl release 69). Arctic ground squirrel (AGS) expressed sequence tags (EST) sequences were generated from EST sequencing project at University of Alaska Fairbanks.[4,5] 24,371 AGS ESTs with a length of 496 (SD ±133) were obtained.

TGS protein sequence correction - To identify and correct AGS specific sites on TGS protein sequences, we mapped translated AGS EST in three frames onto TGS protein sequences by BLAT[6] with default parameters. The EST was considered as the protein homolog if the alignment identity was >70%. Such EST-protein pairs were selected for correction, involving 7,308 proteins and 15,029 ESTs (Table S2). For each protein, the entire sequence was scanned for mismatched sites, which were then replaced by the amino acid that occurred most frequently in the same position of the ESTs (Figure S2). If more than one amino acids tied, we recorded the one from the EST that had the highest identity with the protein. 5,658 protein sequences were corrected through this process, and 2.7% of their sites were changed on average.

Alignment of the remaining ESTs and human protein sequences - To collect information embedded in ESTs that failed to align onto TGS sequences, we further used BLAST to align them onto human protein sequences. Alignments with >70% identity were taken into consideration, involving 1,842 proteins and 986 ESTs (Table S3). Mismatches were corrected as described in Figure S2. The alignment region was extracted as AGS peptide (Figure S3). If more than one EST mapped onto the same protein, the gaps between ESTs were closed using the human protein sequences. 1,842 AGS peptides resulted from this process, with length of 100 (SD ±118). The coverage, corrected proportion, and gap proportion of those peptides are shown in Figure S4. Only a few peptides have large proportion of gaps.

Final AGS protein database composition - the refined protein database for AGS included the whole length of 20,000 sequences in TGS with corrected sites, and 1,842 sequences of peptides aligned with human proteins.

1.C.2. Results of protein database searches. Appended to each database was a reversed-sequence "decoy" of each protein for false positive rate determination. Included in the database searches were variable modifications on methionine (oxidation) and Asn/Qln (deamidation). After individual peptide scoring using PeptideProphet algorithm (Elucidator), the data was annotated at a <1% peptide false discovery rate. This analysis yielded identifications for 8733 peptides/1337 proteins across all rat samples and 9733 peptides/1520 proteins across all AGS samples. Although the QC pool samples were a conglomerate of both rat and AGS samples, the data were searched against just the AGS database and yielded 4905 peptides/885 proteins. For quantitative processing, the data was first curated to contain only high quality peptides with appropriate chromatographic peak shape, peptide quantities across all five LC/LC fractions were summed, and the dataset was intensity scaled to the robust mean across all samples analyzed; the final quantitative dataset for the rat data was based on 8482 peptides/**1320 proteins** (786 proteins contained at least 2 unique peptides), the AGS data was based on 5250 peptides/**1154 proteins** (806 proteins contained at least 2 unique peptides; 1133 mapped onto TGS Ensembl Protein ID and 21 onto Human Ensembl Protein IDs), and for the QC pool data was based on 4873 peptides and contains 882 proteins (526 proteins contained at least 2 unique peptides).

1.D. Quality control of proteomic datasets.

1.D.1. Outlier Screening. To screen for potential outliers, each individual sample within an experimental definition was plotted on a Principal Component Analysis (PCA) plot for the top three principal components based on z-scored transformed (measurement of the significance of change) protein intensity. For AGS samples, PCA resulted in a fairly equal distribution of points across the 3D space, with no obvious outliers. For rat, two samples, CA174 (R3h) and CA177 (R3h), were significantly separated from all others on Principle Component 1 (the most significant component). A brownish color was also noted upon addition of the Trizol reagent during preparation for these two samples, suggesting blood contamination. To confirm the disproportionate contribution from blood in these samples, we plotted the intensities of hemoglobin alpha subunit and hemoglobin beta subunit. Although it would be possible to simply remove the signals from the hemoglobin and renormalize the data without these proteins, there is very likely a host of other high abundant serum proteins from the blood that would also be artificially skewed. This was visualized by performing a two-dimensional agglomerative cluster of all protein intensities within just the five rat R3h samples. Clearly, there are a significant number of proteins (~ 1/3) that have a different expression profile than the other three R3h samples. Based on this quality control data, we decided to exclude these samples altogether from any type of downstream statistical analyses.

1.D.2. Technical reproducibility and intra-experimental group biological variation. To assess system reproducibility, the non-intensity scaled protein-level expression data for yeast alcohol dehydrogenase (ADH) spiked at the same quantity into each of the samples revealed a protein intensity coefficient of variation (% RSD) of 21.1% across all rat samples (outliers excluded), 13.3% across all AGS samples and 15.9% across all QC pool samples. These values are all within expected system variation levels commonly observed for a study of this size (46 samples with 12 days of uninterrupted instrument acquisition) and indicate a consistent analytical performance across over that time. To further interrogate the system reproducibility, the variation in protein intensity from all 882 proteins identified in the 8 QC pool samples was measured. Average coefficients of variation in protein intensity were 10.9% with a median of 7.6% across the 882 proteins. If only proteins with at least two unique peptides were included, the average variation in protein intensity was lowered to 7.2% across the 526 proteins. As with the ADH internal standard, these reproducibility metrics indicate a high degree of analytical reproducibility. The average biological variation within each treatment group was also calculated. On average, the rat samples had less variation (% coefficient of variation) in a protein's abundance within an experimental group than any of the AGS treatment groups. As expected, the average variation of proteins within the QC pool samples was significantly lower than either of the individual animal groups.

1.E. Arctic ground squirrel to rat orthology mapping. A key component of our analytical strategy to compare changes in myocardial protein expression across species involves the establishment of orthologous relationships among the proteins identified and quantified using label-free proteomic approaches in rat vs AGS. Commonly used methods for orthology assessment typically use BLAST to search for pairs of reciprocal

best hits in the genomes (or proteomes) being compared. However, these methods are easily misled when additional duplications occur after the species in question have diverged ("in-paralogs"), leading to the presence of co-orthologs in cross-genome comparisons. We have defined sets of putatively orthologous genes/proteins among those identified within each species by 5-fraction 2D-LC/LC-MS proteomics. These orthologies were established by adapting the EnsemblCompara GeneTrees resource developed by Vilella *et al*,[7] a system that automates the clustering, multiple alignment, and phylogenetic analysis necessary to build gene trees for large numbers of gene families represented in the Ensembl project. We believe that an explicitly phylogenetic approach is necessary for accurate orthology assessment and distinguishing co-orthologs from paralogs (unlike traditional reciprocal BLAST and other non-phylogenetic methods). Given the known one-to-one, one-to-many and many-to-many orthology relationships, we used the BioMart data-mining tool (available at http://www.ensemble.org) and Ensembl Genes Release 73 (Rnor_5.0 for rat, Spetri2 for squirrel) to conduct a bidirectional orthology matching using first the rat as the reference genome and then the AGS as the reference genome.

Rat→AGS orthology mapping: of the 1320 unique rat GI protein accession numbers, 46 had no rat Ensembl Protein ID and/or no squirrel orthologs available. Of the remaining 1274 GI protein accession numbers, 181 had more than one Ensembl Protein ID (splice variants etc), resulting in 1563 Ensembl Protein IDs. Due to one-to-many and many-to-many relationships, this corresponded to 1518 rat-squirrel ortholog pairs, involving 1315 out of the 1563 unique rat Ensembl Protein IDs (1108 of the 1274 unique rat GI accession numbers) and 1180 unique squirrel Ensembl Protein IDs. The final ***rat→AGS*** orthology map file contains 1222 unique rat GI-squirrel Ensembl Protein ID ortholog pairs, corresponding to the 1108 unique rat GI accession numbers and 1180 unique squirrel Ensembl Protein IDs (59 rat GI accession numbers mapped to >1 squirrel Ensembl IDs). However, not all 1180 squirrel proteins in the rat-AGS orthology map were identified and quantified in the myocardial samples. Restricting the map to the 1154 AGS proteins identified yielded 623 unique rat GI accession numbers mapped to 615 unique squirrel Ensembl IDs. A summary of this process is provided in Figure S1.

Figure S1. Computational approach to establish an orthology map between the two species using Ensembl Compara

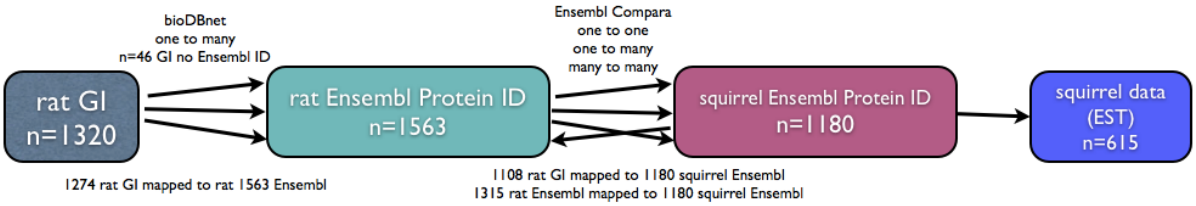

AGS→rat orthology mapping: of the 1154 unique AGS proteins identified using the EST protein database search, 1133 were matched onto TGS (*Ictidomys tridecemlineatus*) Ensembl Protein IDs and 21 matched onto Human Ensembl Protein IDs. Of the 1133 TGS protein IDs, 1113 were mapped to rat orthologs (20 squirrel genes did not have rat orthologs based on EnsemblCompara). Of the 21 human protein IDs, 20 had rat orthologs (one to one or one to many), resulting in 30 ortholog pairs. The final ***AGS→rat*** orthology map contains 2037 ortholog pairs, corresponding to 1133 unique squirrel/human protein IDs mapped to 1867 unique Rat protein IDs. The 1867 unique rat Ensembl IDs were restricted to the 1320 identified in the myocardial samples, resulting in 687 AGS-rat orthology pairs.

The *rat→AGS* and *AGS→rat* orthology files were finally merged into a single orthology map - containing 702 unique rat GI protein IDs, 700 unique squirrel (or human) Ensembl Protein IDs, and 697 unique gene names – which was used for downstream cross-species comparative analyses of myocardial protein abundance.

1.F. Pathway analysis workflow using MetaCore. MetaCore (Thomson Reuters, Philadelphia, PA) is an integrated software suite for functional analysis of proteomic data. Canonical pathway maps represent a set of signaling and metabolic maps covering various model organisms in a comprehensive way. All maps are created by Thomson Reuters scientists, through a high-quality manual curation process based on published peer-reviewed literature. Experimental data is visualized on the maps as blue (for downregulation) and red (upregulation) histograms. The height of the histogram corresponds to the relative expression value for a

particular gene/protein. Biological interpretation of differentially expressed protein lists was conducted using enrichment analysis in MetaCore v6.15. After individual protein IDs were mapped onto functional ontologies in MetaCore (canonical pathway maps, GO processes, and process networks), the probability of a random intersection between a set of IDs the size of the target protein list with ontology entities is estimated as the p-value of a hypergeometric intersection. Thus, a lower p-value means higher relevance of the entity to the dataset. The compare experiments workflow in MetaCore was used to investigate the biological significance of changes unique to each species or hibernation state.

1.G. Mitochondrial DNA analysis and quantitative real-time PCR. The relative copy number of mtDNA per diploid nuclear genome was calculated in each species/experimental group by quantitative RT-PCR as a biomarker of mitochondrial content in the cardiac muscle. Total DNA was extracted from rat and AGS LV myocardium using a QIAamp DNA Mini Kit, and the ratio of a mitochondrial-encoded gene (*Cytochrome c oxidase, subunit I, Mt-Co1*) vs. a nuclear-encoded gene (*Cyclophilin A, Ppia*) was determined by RT-PCR as described.[8] Sequences for the real-time primers and Taqman probes for the rat *Mt-Co1* and *Ppia* genes are commercially available (Rn03296721_s1; Rn00690933_m1) generating amplicons of 94 bp and 149 bp, respectively. Real-time PCR primers and probes for the AGS *Mt-Co1* and *Ppia* genes were designed using the custom Taqman assay design tool (Life Technologies, Grand Island, NY) with sequences identified from NCBI or provided by Dr. Anya Goropashnaya, Institute of Artic Biology, University of Alaska, Fairbanks. For *Mt-Co1* gene fragment amplification, the primers were: 5'-CTTTCCTTCTCTTACTCGCTTCTTCT-3' (forward) and 5'-CGGCTAATGGAGGATAAACAGTTCA3' (reverse), and the TaqMan probe was 5'-CCTGCACCTGCTTCAA-3' (88 bp amplicon). For *Ppia* gene fragment amplification, the primers were 5'-AGGGTTCCTGCTTTCACAGAATT-3' (forward) and 5'-GCCATTATGGCGTGTGAAGTC-3' (reverse), and the TaqMan probe was 5'-CCACCCTGGCACATAA-3' (71 bp amplicon). The total reaction volume was 20 µl and contained: 10 µl 2×TaqMan® Universal Master Mix II, no UNG (Life Technologies), 10 ng template DNA, and 1 µl of each Taqman gene expression assay primer/probe mix. The quantitative RT-PCR reactions for rat and AGS *Mt-Co1/Ppia* were run on the same 96 well plate, in triplicate, with a thermal cycling program as follows: 50°C for 2 min and 95°C for 10 min, followed by 40 cycles of 95°C for 15 s and 60°C for 1 min. The RT-PCR was performed in a StepOnePlus Real-Time PCR System (Life Technologies), and data analyses were based on measurement of the cycle threshold (Ct) using StepOne v2.2.3 software.

1.H. Western blot analysis. Cardiac tissue homogenates were subjected to BCA assay for protein quantification. Following SDS PAGE electrophoresis using the Criterion Electrophoresis System (Bio-Rad), gels were equilibrated with Tris/glycine/10% methanol for 15 minutes and transferred to PVDF using the Criterion Gel-Blot System (Bio-Rad). Blots were blocked for 1 hr in SuperBlock T20 (TBS) Blocking Buffer (Thermo Scientific). All antibodies were diluted in SuperBlock T20, at concentrations specified by their supplier, and blots were incubated overnight at 4°C with gentle rocking. Primary antibodies included: anti-NDUFS8 (V-15, sc243594 goat polyclonal, Santa Cruz Biotechnology) anti-SDHA (2E3GC12FB2AE2, ab14715 mouse monoclonal, Abcam Inc.), anti-COX5A (6E9B12D5, ab110262 mouse monoclonal, Abcam Inc.), anti-UQCRQ (1H9DE5DG5BC8, ab110255 mouse monoclonal, Abcam Inc.), anti-ATP5A (15H4C4, ab14748 mouse monoclonal, Abcam Inc.), anti-COX IV (3E11, #4850 rabbit monoclonal, Cell Signaling Technology), anti-Hsp60 (EP1006Y, ab45134 rabbit monoclonal, Abcam Inc.), and anti-βactin (Sigma A3854 monoclonal, clone AC-15). After washing with TBS-T, to remove unbound primary antibody, blots were incubated with secondary, HRP conjugated antibodies, diluted in SuperBlock T20, for 1 hr at room temperature. Blots were washed 4 times with 40-50 ml of TBS-T over 5 min and binding of HRP conjugated, secondary antibody was detected using SuperSignal West Pico Substrate (Pierce), as recommended by the manufacturer. COX-IV was used for loading control for the lower molecular weight proteins NDUFS8, UQCRQ and COX5A, whereas HSP60 us used as loading control for the higher molecular weight proteins SDHA and ATP5A. Primary antibody dilutions were 1:1000, and secondary antibodies were at 1:10,000. Membranes were developed with a chemiluminescent system (FluorChem HD2 System, Alpha Innotech) and analyzed with AlphaView v. 3.4.0.0. software. For presentation purposes, images may have had background subtraction and linear adjustments to scale intensity; however, unless stated images on a single blot were adjusted simultaneously to maintain signal intensity relationships.

1.I. Targeted metabolic profiling. A 50-mg piece of snap-frozen LV tissue was cut and placed on dry ice, and 250 µL of ice cold homogenizing solvent was added (50% aqueous acetonitrile containing 0.3% formic acid). A hand-held homogenizer with a 7-mm head was used to liquefy the tissue for approximately 25 seconds. Samples were analyzed at the Duke Molecular Physiology Institute by tandem mass spectrometry optimized for detection of targeted metabolites, which included acylcarnities, organic acids, amino acids and ceramides (the Stedman platform). The data was acquired using a Waters Acquity UPLC system equipped with a triple quadrupole detection and a data system controlled by MassLynx 4.1 operating system (Waters, Milford, MA).

1.J. Nuclear receptor activity assay. A 500-mg piece of the left ventricle was cut on dry ice and used to generate nuclear extracts with the Panomics nuclear extraction kit, according to manufacturer's specifications (Fremont, CA). PPAR-α nuclear receptor activity was assessed in the nuclear fraction by ELISA (Affymetrix, Santa Clara, CA). Briefly, ELISA plates with immobilized DNA for the PPAR-α responsive element were loaded with nuclear extract. These plates were allowed to incubate and then washed so that only activated nuclear receptor protein would be bound to its specific responsive element. Colorimetric change was then detected by antibodies specific for DNA/nuclear receptor protein complexes.

2. SUPPLEMENTAL RESULTS

2.A. The cardioprotective hibernator phenotype. Myocardial apoptosis following experimental surgical I/R was attenuated in hibernating AGS compared to rats, as evidenced by reduced fractions of cardiomyocytes staining positive for active caspase-3 (Figure S2.A) and number of TUNEL-positive cells (Figure S2.B).

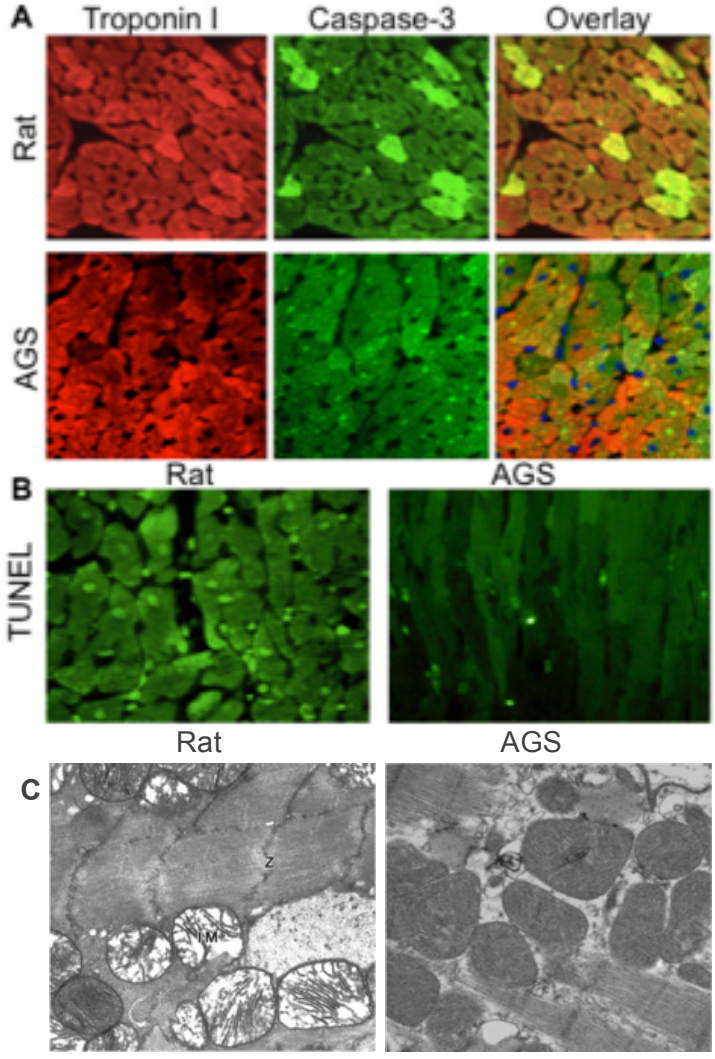

Figure S2. Immunofluorescence microscopy performed on formalin-fixed sections of LV at 3h post-reperfusion demonstrating increased numbers of caspase-3 positive cardiomyocytes in rats compared to hibernating AGS (A), and increased number of TUNEL positive nuclei (B). Electron micrographs at 3h post-reperfusion reveal normal appearing myocytes in AGS with intact mitochondrial ultrastructure, whereas rat cardiomyocytes had swollen mitochondria and irregularly arranged myofibrils (C). (x27,000)

2.B. Principal component analysis across all samples was performed using Partek Genomics Suite v6.6 (Partek, Inc, St Louis, MO). The most significant separation along PC1 occurred between species (AGS vs rat), with hibernation state (hibernating vs summer active AGS) and reperfusion timepoints (sham vs R3h vs R24h) contributing little to the sources of variation across the experimental dataset (Figure S3).

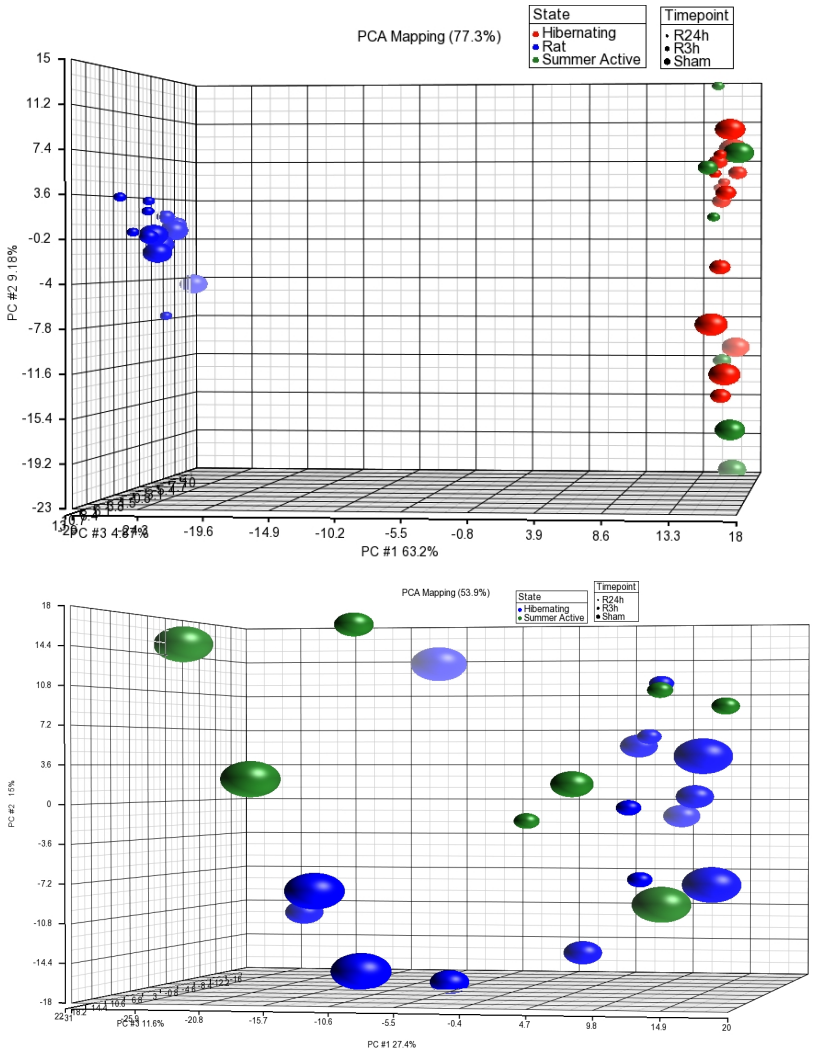

Figure S3. PCA plots by species (AGS vs rat), hibernation state and timepoint (*top*), and by hibernation state (AGS only) and timepoint (*bottom*). Color – species and hibernation state; size – reperfusion timepoint

Sources of experimental variation were identified by plotting signal vs noise across all orthologous proteins for each of the factors and interactions in the mixed model ANOVA (displayed on the x-axis, including random error). Average mean square (ANOVA's measure of variance) across all proteins is represented on the y-axis. All bars are higher than the error bar, thus all factors contributed significant variation to the data across the set, with species (AGS vs rat) representing the dominant source of variation (Figure S4).

Figure S4. Sources of Variation

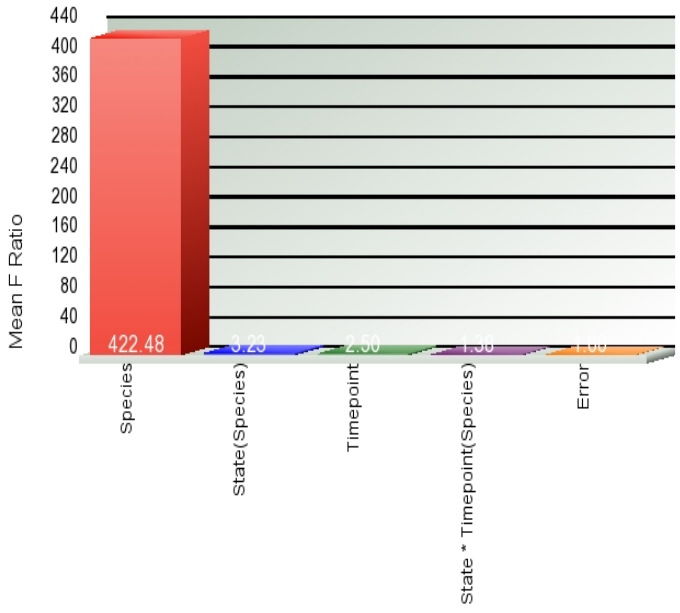

2.C. Cross-species hibernating AGS (HIB) vs. rat comparisons

A volcano plot of global proteomic changes between HIB and Rat is presented in Figure S5.

Figure S5. Volcano Plot of Overall Hibernating AGS vs Rat Protein Differences

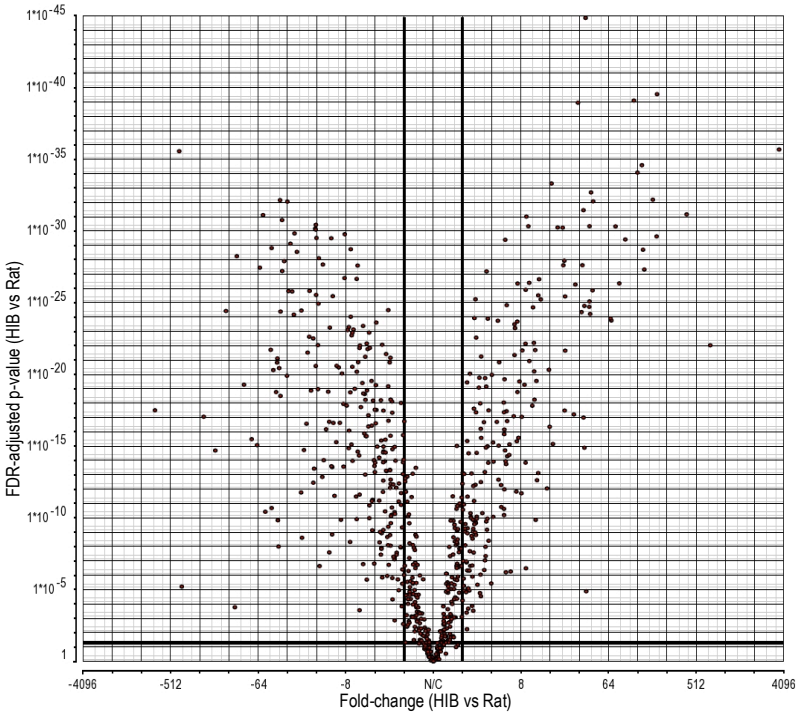

2.C.1. The 290 proteins downregulated in HIB vs rat (HIB<Rat) mapped onto canonical pathways involved in mitochondrial function, energy metabolism, and immune responses (Figure S6). The top pathway map based on the enrichment distribution involves downregulation of proteins involved in the electron transport chain (ETC).

Figure S6. Top pathway maps sorted by significance based on the enrichment distribution in HIB<Rat

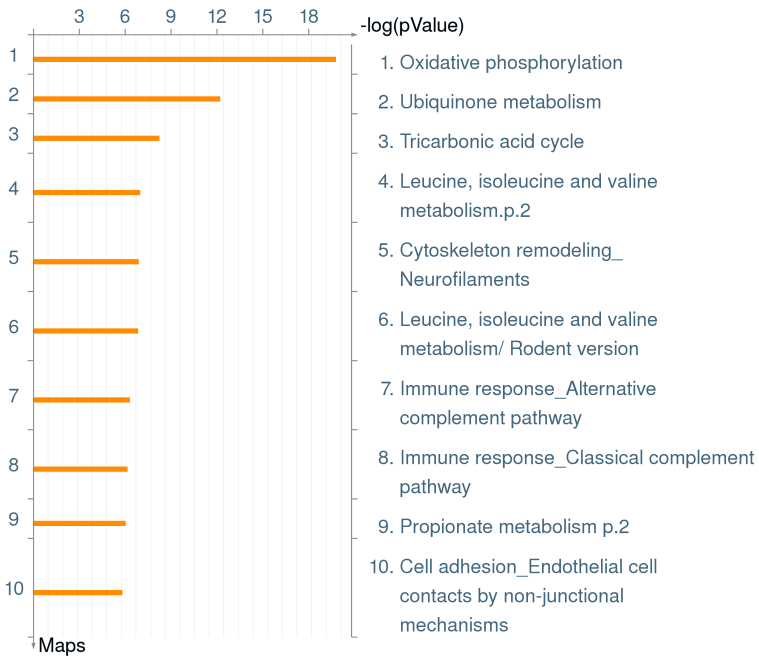

Furthermore, the protein content of the uploaded files is used as the input for generation of biological networks using Analyze Networks algorithm in MetaCore. This is a variant of the shortest paths algorithm with main parameters of relative enrichment with the uploaded data and relative saturation of networks with canonical pathways. The networks are then prioritized based on the number of fragments of canonical pathways on the network. The most relevant network in HIB<Rat involved MyD88-dependent toll-like receptor (TLR) signaling pathway (56%), TLR1 signaling pathway (54%), positive regulation of defense response (70%), TLR6:TLR2 signaling pathway (54%), TLR1:TLR2 signaling pathway (54%).

2.C.2. The 255 proteins upregulated in HIB vs rat (HIB>Rat) mapped onto canonical pathways involved in fatty acid metabolism, RNA metabolic processes, protein synthesis-translation elongation, cytoskeleton remodeling, and antigen presentation by MHC class I (Tables S1-S3).

Table S1. Members of the RNA metabolism pathway upregulated in hibernating AGS vs rat

Protein symbol	Protein name	FC HIB vs Rat	FDR adjusted p-value
Hnrpd	Heterogeneous nuclear ribonucleoprotein D0	6.57	6.98E-17
Hspa1b	heat shock 70kD protein 1B (mapped)	5.55	3.08E-25
Lsm3	LSM3 homolog, U6 small nuclear RNA associated	2.56	1.95E-06
Pcbp2	poly(rC) binding protein 2	38.79	3.09E-16
Psma2	Proteasome subunit alpha type-2	19.21	4.33E-26
Psma6	Proteasome subunit alpha type-6	5.55	7.43E-13
Psmb1	Proteasome subunit beta type-1 (26S proteasome)	2.21	8.29E-06
Psmb5	Proteasome subunit beta type-5	3.62	8.28E-15
Psmb6	Proteasome subunit beta type-6	8.51	7.33E-20
Psmc3	26S protease regulatory subunit 6A	36.27	5.26E-21
Psmc4	26S protease regulatory subunit 6B	7.20	2.52E-16
Psme3	proteaseome (prosome, macropain) 28 subunit, 3	7.88	2.60E-17
RGD1559955	Small 40S subunit	3.55	1.67E-14
Rpl11	60S ribosomal protein L11	2.56	1.85E-09
Rpl13	60S ribosomal protein L13	2.67	3.04E-12
Rpl14	60S ribosomal protein L14	9.62	3.92E-27
Rpl15	60S ribosomal protein L15	11.65	1.28E-19
Rpl18	60S ribosomal protein L18	2.55	4.48E-09
Rpl23	60S ribosomal protein L23	2.35	2.06E-06
Rpl23a	60S ribosomal protein L23a	1.27	1.13E-03
Rpl24	60S ribosomal protein L24	3.50	1.01E-14
Rpl27	60S ribosomal protein L27	1.78	4.29E-06
Rpl35a	60S ribosomal protein L35a	50.12	3.67E-07
Rpl36al	60S ribosomal protein L36a	1.32	1.43E-02
Rpl6	60S ribosomal protein L6	2.16	6.54E-09
Rplp1	60S acidic ribosomal protein P1	8.52	1.55E-11
Rps12	40S ribosomal protein S12	1.95	7.08E-08
Rps18	40S ribosomal protein S18	1.27	2.33E-05
Rps29	40S ribosomal protein S29	5.10	1.06E-11
Rps7	40S ribosomal protein S7	2.63	1.28E-18
Rpsa	40S ribosomal protein SA	3.49	6.56E-24

Table S2. Members of the protein synthesis-translation elongation pathway upregulated in hibernating AGS vs rat

Protein symbol	Protein name	FC HIB vs rat	FDR-adjusted p value
Eef1a1	Elongation factor 1-alpha 1	16.81	8.41E-31
Eef1b2	eukaryotic translation elongation factor 1 beta 2	44.27	2.61E-23
Eef1d	Elongation factor 1-delta	1.45	6.33E-07
Eef1g	Elongation factor 1-gamma	116.44	3.16E-35
Eef2	Elongation factor 2	2.26	1.07E-03
Gfm1	Elongation factor G, mitochondrial	3.99	1.39E-05
RGD1559955	similar to 40S ribosomal protein S17	3.55	1.67E-14
Rpl11	60S ribosomal protein L11	2.56	1.85E-09
Rpl13	60S ribosomal protein L13	2.67	3.04E-12
Rpl14	60S ribosomal protein L14	9.62	3.92E-27
Rpl15	60S ribosomal protein L15	11.65	1.28E-19
Rpl18	60S ribosomal protein L18	2.55	4.48E-09
Rpl23	60S ribosomal protein L23	2.35	2.06E-06
Rpl23a	60S ribosomal protein L23a	1.27	1.13E-03
Rpl24	60S ribosomal protein L24	3.50	1.01E-14
Rpl27	60S ribosomal protein L27	1.78	4.29E-06
Rpl35a	60S ribosomal protein L35a	50.12	3.67E-07
Rpl36al	60S ribosomal protein L36a	1.32	1.43E-02
Rpl6	60S ribosomal protein L6	2.16	6.54E-09
Rplp1	60S acidic ribosomal protein P1	8.52	1.55E-11
Rps12	40S ribosomal protein S12	1.95	7.08E-08
Rps18	40S ribosomal protein S18	1.27	2.33E-05
Rps29	40S ribosomal protein S29	5.10	1.06E-11
Rps7	40S ribosomal protein S7	2.63	1.28E-18
Rpsa	40S ribosomal protein SA	3.49	6.56E-24

Table S3. Members of the cytoskeleton remodeling pathway upregulated in hibernating AGS vs rat

Protein symbol	Protein name	FC HIB vs Rat	FDR adjusted p-value
Ablim1	actin-binding LIM protein 1	1.27	2.79E-03
Acta2	smooth muscle alpha-actin	31.20	9.07E-35
Cfl2	cofilin 2, muscle	6.88	2.28E-21
Col4a2	collagen, type IV, alpha 2	3.70	1.01E-15
Col6a1	collagen, type VI, alpha 1	1.74	1.42E-06
Col6a2	collagen, type VI, alpha 2	2.37	1.71E-18
Dag1	dystroglycan 1 (dystrophin-associated glycoprotein 1)	1.61	7.01E-05
Dctn2	dynactin 2 (p50)	2.75	1.40E-10
Des	desmin	1.65	8.13E-09
Dpysl2	dihydropyrimidinase-like 2	-12.37	6.74E-08
Dsg2	desmoglein 2	1.52	1.64E-02
Dstn	destrin	4.97	5.36E-16
Eif4h	eukaryotic translation initiation factor 4H	1.18	7.35E-03
Fam82b	regulator of microtubule dynamics 1	2.17	3.01E-09
Gja1	gap junction protein, alpha 1 (connexin-43)	2.35	5.80E-06
Lama2	laminin, alpha 2	1.37	3.87E-06
Lama5	laminin, alpha 5	6.16	8.57E-14
Lamb2	laminin, beta 2	1.52	4.01E-05
Lmna	lamin A/C	2.70	3.25E-22
Myh13	myosin, heavy chain 13, skeletal muscle	1.60	1.16E-04
Myl10	myosin, light chain 10, regulatory	3441.81	4.38E-32
Myl2	myosin, light chain 2, regulatory, cardiac, slow	1.77	6.91E-09
Plg	plasminogen	1.54	6.32E-04
Prph	peripherin	2.14	7.78E-10
Sgcd	sarcoglycan, delta (dystrophin-associated glycoprotein)	1.28	1.39E-02
Sptbn1	spectrin, beta, non-erythrocytic 1 (beta-fodrin)	3.26	1.39E-07
Tubb4b	tubulin, beta 4B class IVb	-2.79	2.25E-21
Tubb5	tubulin, beta 5 class I	1.69	3.79E-07
Vcl	vinculin	34.47	2.06E-15
Vim	vimentin	1.66	6.89E-06

2.C.3. Comparisons HIB vs Rat by experimental timepoint. A Venn diagram of the overlap between differentially expressed proteins between HIB and rat in sham, R3h and R24h groups is presented in Figure S7. Few proteins were uniquely differentially expressed both early (R3h) and late (R24h) post reperfusion. Oxidative phosphorylation (ATPsynthase, Uqcrqpc, Uqcrb, Atp5c) and cell adhesion-cytoskeletal remodeling (laminin 1, 2, 4, 8, MyHC, Myosin II) pathways were significantly enriched at both reperfusion timepoints. Dynamic responses in myocardial protein abundance following I/R were assessed in each species at 3h and 24h post-reperfusion relative to sham controls. At R3h, 14 proteins were differentially expressed in HIB and 9 proteins in rat, with no cross-species overlap. At R24h, 61 proteins were changed in HIB and 84 in rat, with 9 proteins being jointly deregulated in both species.

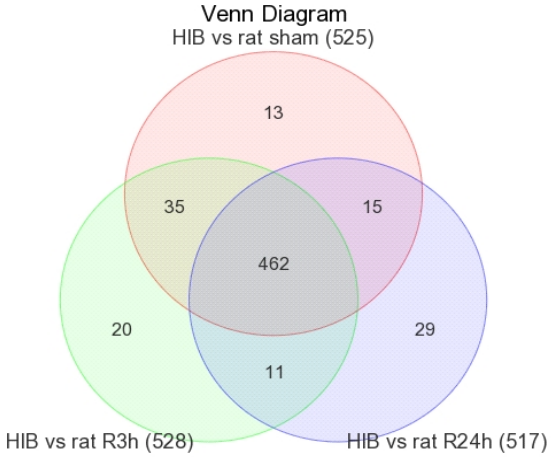

Figure S7. HIB vs Rat comparisons by experimental group and timepoint

The results of comparative cross-species pathway analysis between differentially expressed proteins at R24h relative to sham are presented below. After the I/R-induced changes in myocardial protein content were aligned between the two species, the intersection set of proteins was defined as 'common' and marked with a blue/white striped bar (Figure S8). The unique proteins for rat and HIB are marked as orange and blue bars, respectively. Enrichment analysis consists of matching protein IDs of possible targets for the 'common', 'similar' and 'unique' sets with gene IDs in functional ontologies in MetaCore. The probability of a random intersection between a set of IDs the size of the target list with ontology entities is estimated as the p-value of a hypergeometric intersection. The lower the p-value the higher the relevance of the entity to the dataset. The top 10 scoring pathway maps sorted by statistical significance are presented in Figure S8 below.

Figure S8. Top scoring pathway maps for differentially expressed proteins at R24h vs sham in HIB and rat, sorted by statistical significance

Among the 52 proteins uniquely differentially expressed at 24h post-reperfusion relative to sham in HIB myocardium (but not in rat), members of the mitochondrial electron transport chain were overrepresented (Table S4).

Table S4. Members of the mitochondrial ETC uniquely deregulated in hibernating AGS (but not rat) myocardium at R24h relative to sham

Protein symbol	Protein name	FC HIB R24 vs HIB sham	FDR adjusted p-value
Complex I			
Ndufa13	NADH dehydrogenase (ubiquinone) 1 alpha subcomplex, 13	-1.78	5.52E-03
Ndufb4	NADH dehydrogenase (ubiquinone) 1 beta subcomplex, 4, 15kDa	-1.64	2.63E-02
Ndufb6	NADH dehydrogenase (ubiquinone) 1 beta subcomplex, 6	-2.65	5.77E-04
Ndufc2	NADH dehydrogenase (ubiquinone) 1, subcomplex unknown, 2	-1.61	4.04E-02
Ndufs3	NADH dehydrogenase (ubiquinone) Fe-S protein 3	-1.44	2.01E-02
Ndufs5	NADH dehydrogenase (ubiquinone) Fe-S protein 5b, 15kDa (NADH-coenzyme Q reductase)	-1.32	2.46E-02
Complex II			
Sdha	succinate dehydrogenase complex, subunit A	-1.45	2.91E-02
Complex III			
Uqcrq	ubiquinol-cytochrome c reductase, complex III subunit VII	-1.54	3.25E-02
Complex IV			
Cox5b	Cytochrome c oxidase subunit 5B, mitochondrial	-1.32	3.98E-03
Complex V			
Atp5f1	ATP synthase, H+ transporting, mitochondrial Fo complex, subunit B1	-1.72	3.51E-02
Atp5o	ATP synthase, H+ transporting, mitochondrial F1 complex, O subunit	-1.40	3.75E-02

Conversely, of the 75 proteins that were uniquely deregulated at 24h post-reperfusion relative to sham in rat only (but not in HIB), integrin mediated cell adhesion and platelet activation/degranulation pathways were enriched (Table S5).

Table S5. Representative proteins uniquely deregulated in rat (but not hibernating AGS) myocardium at R24h relative to sham

Protein symbol	Protein name	FC RAT R24 vs RAT sham	FDR adjusted p-value
Integrin mediated cell-matrix adhesion			
Fgg	Fibrinogen gamma chain	2.36	9.10E-05
Fgb	Fibrinogen beta chain	1.98	5.18E-03
Ezr	Ezrin	1.92	1.07E-02
Gja1	Gap junction alpha-1 protein (connexin 43)	1.80	2.53E-02
Itgb1	Integrin beta-1	1.33	1.19E-02
Pfn1	Profilin-1	-1.31	2.32E-02
Lama5	Laminin, alpha 5	-1.78	1.24E-02
Platelet activation-degranulation			
Serping1	Plasma protease C1 inhibitor	3.81	4.24E-03
Fgg	Fibrinogen gamma chain	2.36	9.10E-05
Fgb	Fibrinogen beta chain	1.98	5.18E-03
Clu	Clusterin	1.88	7.00E-04
Apoa1	Apolipoprotein A-I	1.55	3.56E-02
Calu	Calumenin	1.31	2.61E-02
Pfn1	Profilin-1	-1.31	2.32E-02
Ywhaq	Tyrosine 3-monooxygenase/tryptophan 5-monooxygenase activation protein, eta polypeptide (14-3-3 protein eta)	-1.39	2.71E-02
Wdr1	WD repeat-containing protein 1	-1.53	1.08E-02

Finally, proteins uniquely differentially expressed among rat at R24h were enriched for myocardial infarction disease biomarkers (FDR adjusted p-value 3.8E-19, Figure S9 and Table S6).

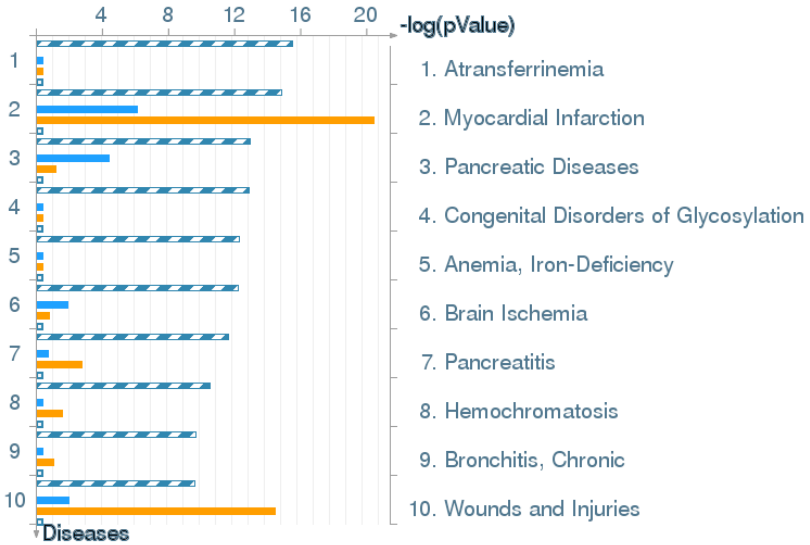

Figure S9. Diseases (by biomarkers) overrepresented among differentially expressed proteins unique to rat R24h relative to sham (rat-orange, HIB-blue bars)

Table S6. Myocardial infarction biomarkers significantly enriched among differentially expressed proteins unique to rat R24h relative to sham

Protein symbol	Protein name	FC Rat R24h vs Rat sham	FDR adjusted p-value
Fgg	Fibrinogen gamma chain	2.36	9.10E-05
Fgb	Fibrinogen beta chain	1.98	5.18E-03
Gc	interleukin 2 receptor, gamma	1.80	4.39E-03
Apoa1	Apolipoprotein A-I	1.55	3.56E-02
Fhl1	complement component factor H	1.50	3.58E-02
Atp5e	ATP synthase, H+ transporting, mitochondrial F1 complex, epsilon subunit	1.38	4.38E-02
Itgb1	Integrin beta-1	1.33	1.19E-02
Anxa5	Annexin A5	1.32	6.25E-03
Atp5a1	ATP synthase, H+ transporting, mitochondrial F1 complex, alpha subunit 1, cardiac muscle	-1.39	3.06E-02
Psmb5	proteasome (prosome, macropain) subunit, beta type 5	-1.45	1.19E-02
Psmb1	proteasome (prosome, macropain) subunit, beta type 1	-2.21	2.31E-03

2.D. Mitochondrial DNA copy number analysis. To ensure that lower abundance of ETC proteins detected in AGS hearts were not secondary to lower mitochondrial content, quantitative real-time PCR was performed to measure copies of mitochondrial cytochrome C oxidase subunit 1 (*Mt-Co1*) and nuclear cyclophilin A (*Ppia*) in rat and AGS (Figure S10). The ratio of mitochondrial gene copy number to nuclear gene copy number was higher for AGS than for rat under all conditions indicating that AGS have an increased number of mitochondria, compared to rat. A decrease in mitochondrial DNA abundance was seen in both species under the R3h condition compared to sham, coincident with peak reperfusion injury.

Figure S10. Real-time PCR was performed for mitochondrial cytochrome C oxidase subunit 1 (*mt-Cox1*) and nuclear cyclophilin A (*Ppia*) in both rat and AGS. A ratio of mitochondrial gene copy number over nuclear gene copy number is presented for rat (**A**) and AGS (**B**) for sham, R3h, and R24h conditions.

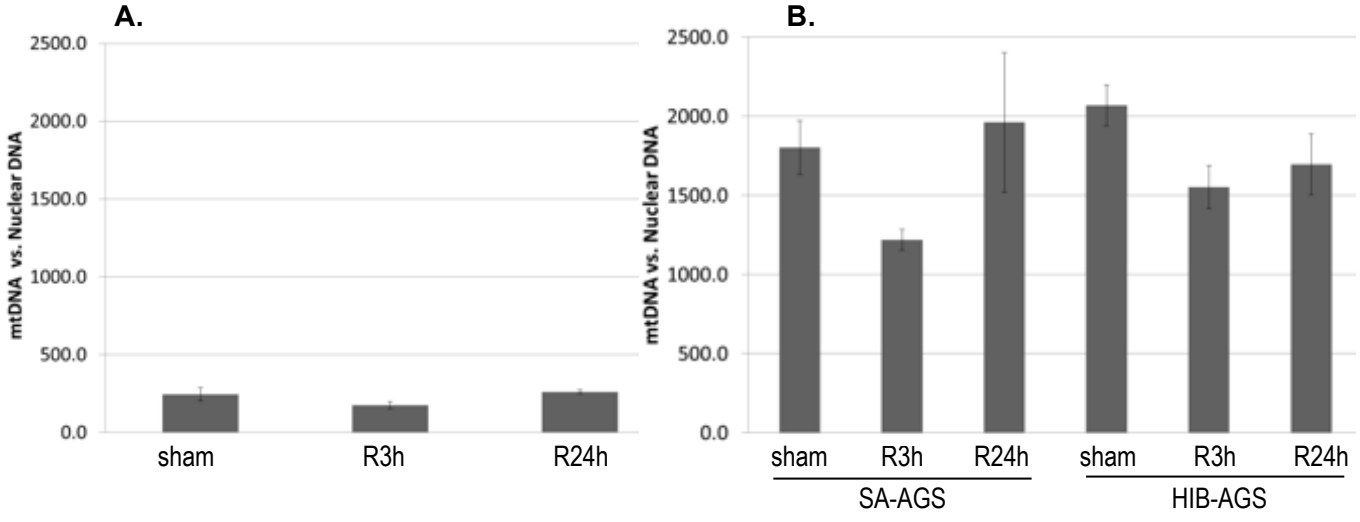

2.E. Western blot validation of mass spectrometry findings was performed for selected electron transport chain proteins. Western blots for NDUFS8 (complex I), COX5A (complex III), and UQCRQ (complex IV), and ATP5A (complex V) for rat, summer AGS, and winter AGS at early reperfusion (R3h) are shown in figure S11. COXIV was used as loading control for the lower molecular weight proteins NDUFS8, COX5a, and UQCRQ (**A**). Densitometric analysis of COXIV normalized bands at R3h timepoint, showing downregulation of NDUFS8, COX5A and UQCRQ in SA-AGS and HIB-AGS relative to rat (**B**). HSP60 was used as loading control for the higher molecular weight protein ATP5A (**C**). Densitometric analysis of HSP60 normalized ATP5A bands at R3h timepoint, showing upregulation in SA-AGS and HIB-AGS relative to rat (**D**).

Figure S11. Western Blots of changes in ETC protein abundance early (R3h) post ischemia-reperfusion by hibernation state in left ventricular myocardium. Panels A, B use COX IV as a loading control, panels C,D use Hsp60. Densitometry results expressed as mean±SEM.

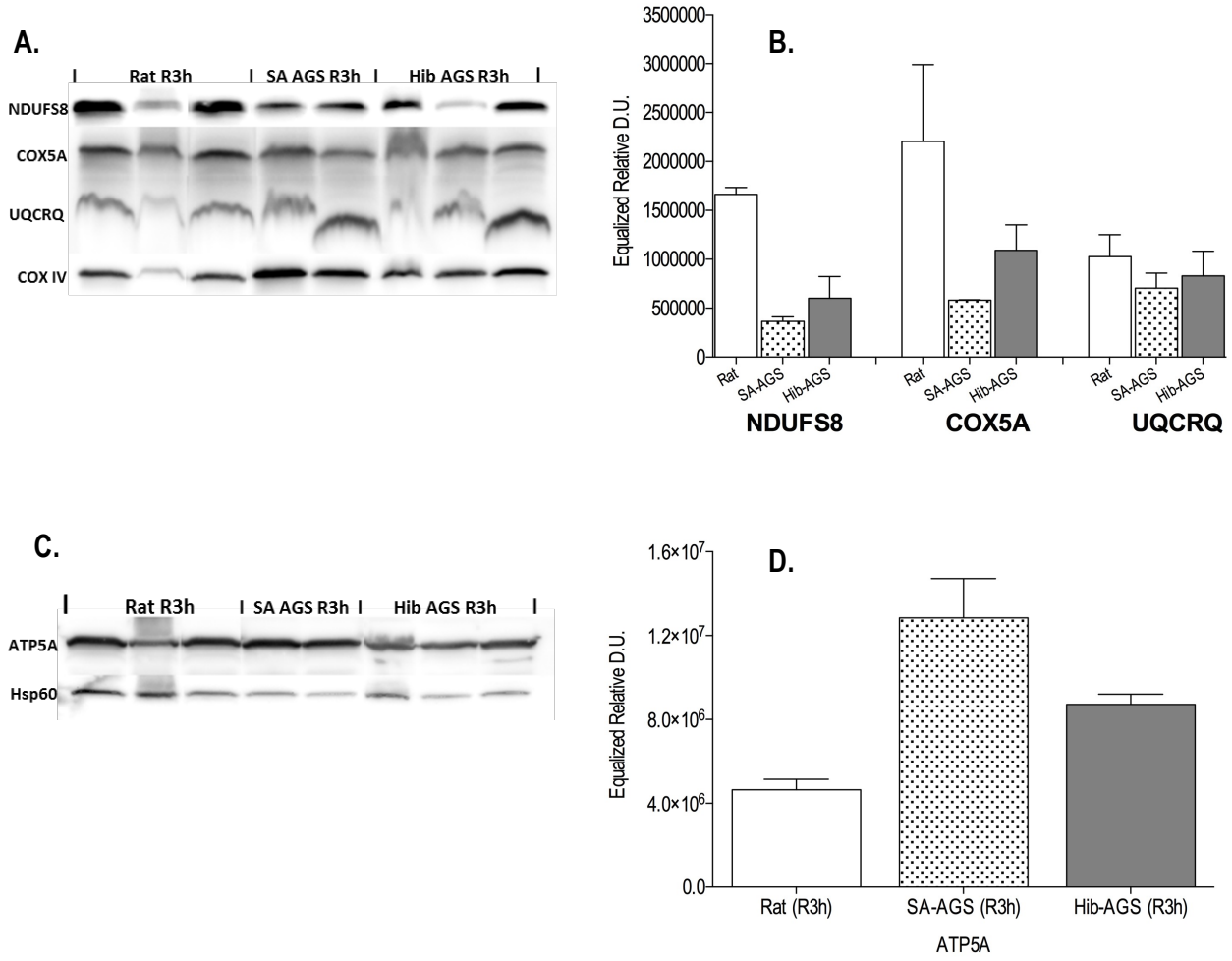

A comparison of fold changes between hibernating AGS and rat hearts in selected electron transport chain, as assessed by mass spectrometry vs. Western blot is presented in Table S7 below.

Table S7.

Protein symbol	Protein name	FC HIB vs Rat Mass Spectrometry	FC HIB vs Rat Western Blot
Complex I (NADH-ubiquinone reductase)			
Ndufs8	NADH dehydrogenase [ubiquinone] Fe-S protein 8	-17.68	-2.76
Complex II (Succinate dehydrogenase-CoQ reductase)			
Sdha	Succinate dehydrogenase complex subunit A	-5.10	-10.99
Complex III (Cytochrome reductase)			
Uqcrq	Cytochrome b-c1 complex subunit 8	-3.57	-1.24
Complex IV (Cytochrome c oxidase)			
Cox5a	Cytochrome c oxidase subunit 5A, mitochondrial	-1.23	-2.02
Complex V (ATP synthase)			
Atp5a1	ATP synthase, H+ transporting, mitochondrial F1 complex, alpha subunit 1, cardiac muscle	**2.24**	**1.88**

2.F. Cardioprotective correlates of Sirtuin-3 upregulation in AGS hearts. Adult primary ventricular cardiomyocytes isolated from rat and AGS were subjected to 2h of oxygen and glucose deprivation, followed by 24h of reoxygenation. Cell viability was assessed by morphometric analysis, as % rod-shaped cardiomyocytes relative to total cells (Figure S12).[9]

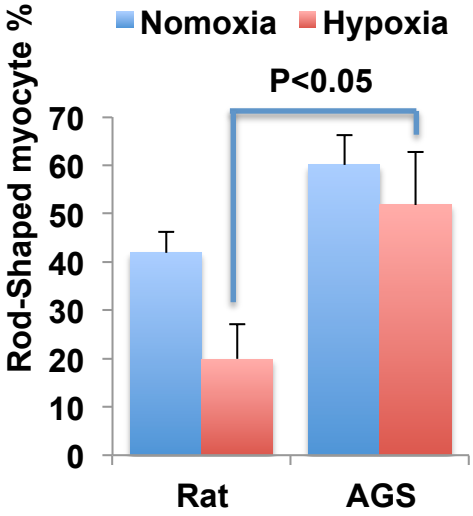

Figure S12. Simulated ischemia-reperfusion via OGD/reoxygenation results in significantly higher cardiomyocyte viability in AGS compared to rat. Data expressed as mean±SD, n=5 replicates.

Following hypoxia-reoxygenation as above, cardiomyocyte mitochondria were isolated using a commercial mitochondria isolation kit for cultured cells (ThermoFisher Scientific, Grand Island, NY) per manufacturer's protocol. Mitochondrial acetylated-lysine proteins (Ac-K-Proteins) were analyzed by Western blot (Figure S13) using Acetylated-Lysine Antibody (Cell Signaling Technology, Danvers, MA) in rats (**A**) and AGS (**B**). COXIV was used as a mitochondrial loading control.

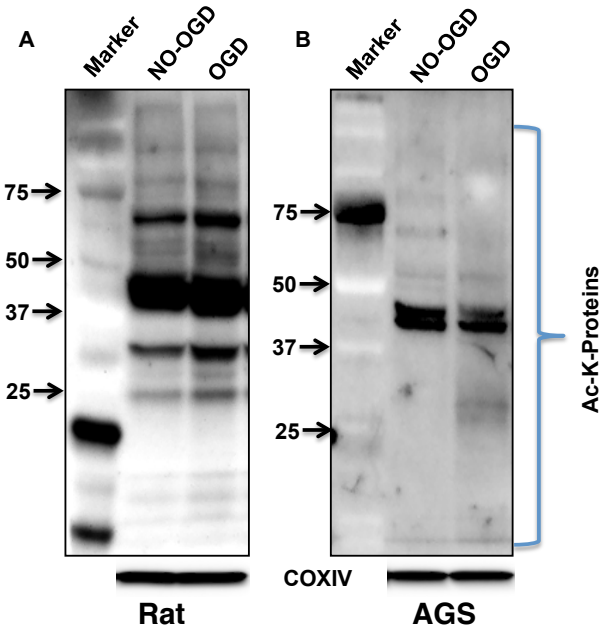

Figure S13. Compared to AGS, rat cardiomyocytes have hyperacetylated mitochondrial proteins, which further increases following hypoxia-reoxygenation. This corroborates the observed increased expression of the major mitochondrial deacetylase SIRT3 in AGS vs rats.

SUPPLEMENTAL REFERENCES:

1. Gilar M, Olivova P, Daly AE, Gebler JC. Orthogonality of separation in two-dimensional liquid chromatography. *Anal Chem.* 2005;77(19):6426-6434.
2. Gilar M, Olivova P, Daly AE, Gebler JC. Two-dimensional separation of peptides using RP-RP-HPLC system with different pH in first and second separation dimensions. *J Sep Sci.* 2005;28(14):1694-1703.
3. Dowell JA, Frost DC, Zhang J, Li L. Comparison of two-dimensional fractionation techniques for shotgun proteomics. *Anal Chem.* 2008;80(17):6715-6723.
4. Fedorov VB, Goropashnaya AV, Toien O, et al. Elevated expression of protein biosynthesis genes in liver and muscle of hibernating black bears (Ursus americanus). *Physiological genomics.* 2009;37(2):108-118.
5. Xu Y, Shao C, Fedorov VB, Goropashnaya AV, Barnes BM, Yan J. Molecular signatures of mammalian hibernation: comparisons with alternative phenotypes. *BMC Genomics.* 2013;14:567.
6. Kent WJ. BLAT--the BLAST-like alignment tool. *Genome Res.* 2002;12(4):656-664.
7. Vilella AJ, Severin J, Ureta-Vidal A, Heng L, Durbin R, Birney E. EnsemblCompara GeneTrees: Complete, duplication-aware phylogenetic trees in vertebrates. *Genome Res.* 2009;19(2):327-335.
8. Miller FJ, Rosenfeldt FL, Zhang C, Linnane AW, Nagley P. Precise determination of mitochondrial DNA copy number in human skeletal and cardiac muscle by a PCR-based assay: lack of change of copy number with age. *Nucleic acids research.* 2003;31(11):e61.
9. Kang PM, Haunstetter A, Aoki H, Usheva A, Izumo S. Morphological and molecular characterization of adult cardiomyocyte apoptosis during hypoxia and reoxygenation. *Circulation research.* 2000;87(2):118-125.